

Coronal activity with XMM-Newton and Chandra

B. Stelzer

INAF - Osservatorio Astronomico di Palermo, Piazza del Parlamento 1, I-90134 Palermo, Italy

Abstract. *XMM-Newton* and *Chandra* have greatly deepened our knowledge of stellar coronae giving access to a variety of new diagnostics such that nowadays a review of stellar X-ray astronomy necessarily must focus on a few selected topics. Attempting to provide a limited but representative overview of recent discoveries I discuss three subjects: the solar-stellar connection, the nature of coronae in limiting regimes of stellar dynamos, and "hot topics" on X-ray emission from pre-main sequence stars.

Keywords: X-rays: stars, Sun: corona, Stars: activity, coronae

PACS: 95.85.Nv, 96.60.P-, 97.10.Bt, 97.10.Ex, 97.10.Jb

THE SOLAR-STELLAR ANALOGY

Ever since the detection of X-ray emission from "normal" stars a comparison of their X-ray properties to those of the Sun has been at the heart of stellar X-ray astronomy. Some of the recent discoveries in investigations of the solar-stellar analogy are the first detection of X-ray activity cycles on stars other than the Sun, studies of the hard X-ray emission during solar and stellar flares, and statistical analysis of flare frequencies.

X-ray activity cycles

Stellar activity cycles have been known to exist from more than 40yrs of monitoring of chromospheric Ca II emission during the Mt. Wilson program [1]. Having in mind that for the Sun, the amplitude of the Ca II variations throughout its 11 yr magnetic cycle is only a factor of two, while the X-ray luminosity of nearby stars varies by a factor of 100, it is reasonable to suspect the existence of coronal activity cycles on solar-like stars. This contrasts with the observation that stars generally show little evidence of long-term X-ray variability. Ca II activity cycles are generally found on relatively inactive stars, while most stars are much more active than the Sun and this might explain their different long-term behavior. Based on these considerations, inactive stars are considered to be the most promising candidates for the detection of X-ray activity cycles. Dedicated *XMM-Newton* monitoring campaigns with snapshot observations on intervals of 6 months have lately provided evidence for systematic long-term variability of the X-ray luminosity in a few nearby stars.

The G-type star HD 81809, to date observed with *XMM-Newton* for a full period of its 8 yr Ca II cycle, displays X-ray variations in accordance with the Ca period (see Fig. 1). Similar to the case of the Sun, the amplitude in X-ray luminosity exceeds that of the

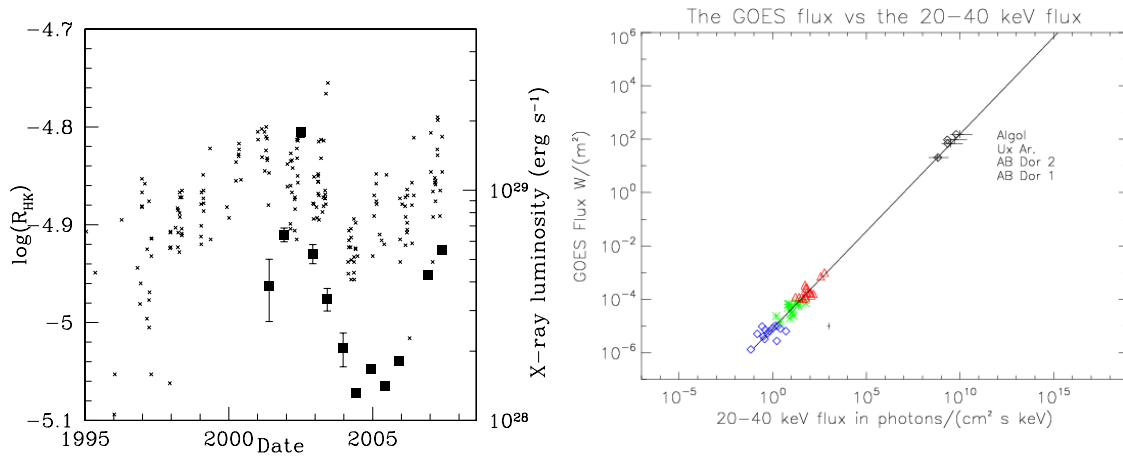


FIGURE 1. *left* - Ca II (small crosses) and X-ray (large circles) activity cycles of the low-activity G star HD 81809 [2]; *right* - Peak flare fluxes at soft and hard X-ray energies for solar and stellar flares [3].

Ca II emission by far. The X-ray luminosity and temperature in different phases of the cycle extend the trend observed in solar data, and can be explained by varying surface coverage with cores of active regions [2]. Direct evidence for X-ray activity cycles from long-term monitoring has been presented for another two stars, α Cen and 61 Cyg [4, 5]. Systematic variability is observed but not enough data has been accumulated to establish a periodic pattern so far.

From the theoretical side, X-ray variability from active stars is predicted on basis of the structure of the coronal magnetic field inferred from an extrapolation of the surface magnetic field maps for the test case AB Dor [6]. The X-ray signal produced by different types of underlying star spot distributions was computed by synthesizing the X-ray emission in closed regions of the estimated coronal field. These simulations show that, depending on the star spot pattern, cyclic variations of the X-ray emission measure may or may not be present. Clearly, from the absence of an X-ray cycle one can not conclude that there is no magnetic cycle.

Soft and hard X-rays in flares

From the standard "thick-target" model for solar/stellar flares one expects a direct causal connection between hard (non-thermal) and soft (thermal) X-ray emission [7]. The relation between the soft and hard peak fluxes of solar flares was studied by [3] using GOES data for the soft emission and RHESSI data for the hard emission. A power-law relation between the peak flux in soft and in hard X-rays was found that holds for over 3 dex of soft X-ray flux from solar flare class C to class X. The *expected* flux relation in the soft and hard emission for a thermal spectrum implies a ~ 6 keV plasma, much hotter than what is observed during solar flares. Therefore, the hard emission was attributed to

a non-thermal origin.

Due to the poor sensitivity for hard X-rays of most stellar X-ray instruments, very few stellar flares have been observed at energies above 10 keV. [3] evaluated the peak fluxes of a handful of stellar flares observed with *BeppoSAX* in the same bands that had been defined for the solar flare observations. Fig. 1 shows that the stellar flares line up almost perfectly along the extrapolation of the Sun's power-law relation between soft and hard peak flare flux. The existence of a unique scaling law for solar and stellar flares underlines that flares are a universal phenomenon.

Flare number energy distributions

The origin of the quiescent X-ray emission of the Sun and the stars has always been a mystery. In absence of a theoretical explanation for the production of persistent X-rays, it has been conjectured that what we observe as apparently quiet might actually be a super-position of small unresolved flares, termed nano-flares because of their $\sim 10^9$ times lower energy compared to the largest solar flares with 10^{33} erg/s [8]. If so, flares are of fundamental importance for the solar coronal heating problem and they may be the actual and the only driver of magnetic activity.

Whether nano-flares are sufficient to come up for the thermal energy budget in the corona of the Sun and the stars depends on their frequency. The number distribution of flares as a function of energy can be approximated by a power-law, $\frac{dN}{dE} \sim E^{-\alpha}$. For a power-law index $\alpha > 2$ the integrated energy of all flares diverges at the low end, and this provides (naively speaking) an infinite heating resource for the corona. For the Sun, [9] observed a frequency distribution of flare energies with a unique slope over eight orders of magnitude in energy [e.g. 9]. However, these results are still disputed and values between $\sim 1.4 \dots 2.6$ have been cited [10, 11].

For stars other than the Sun in general there is no sufficient database for statistical flare studies. A remedy is to look at a sample of stars that can be assumed to be similar, e.g. in an open cluster or in a star forming region, and analyse their collective flare frequency. Recent comprehensive X-ray surveys in star forming regions have been exploited for this purpose. In particular, flare number energy distributions have been evaluated for Orion and Taurus making use of two deep X-ray exposures, the *Chandra Orion Ultradeep Project* (COUP) and the *XMM-Newton Extended Survey in the Taurus Molecular Clouds* (XEST), respectively; see [12, 13] for details on these surveys.

Fig. 2 shows the cumulative distribution of flare energies for two samples of pre-main sequence (pre-MS) stars in Orion and in Taurus. The power-law index is evaluated from the high-energy part of the distribution ($E > E_{\text{cutoff}}$), which is not affected by incompleteness due to the sensitivity limit. This study came up with $\alpha \sim 2$ for both samples, supporting the nano-flare heating hypothesis but with uncertainties that do not exclude a flatter distribution [14]. A number of biases regarding the sensitivity to the detection of flares need to be taken into account: (i) short observations of variable stars are likely not to recover the true base level, and consequently the sensitivity for detecting flares is reduced; (ii) the ability to detect flares differs for stars of different mass, because higher-mass stars are brighter in X-rays, and brighter (i.e. more active)

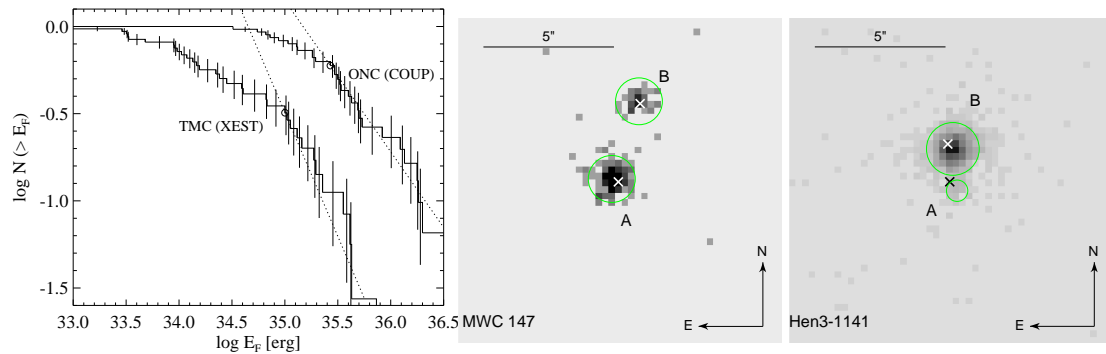


FIGURE 2. *left* - X-ray flare energy number distributions for two samples of pre-MS stars in Taurus and Orion with bestfit power-laws [14]; *middle and right* - *Chandra* images of two Herbig stars (labeled 'A') and their known late-type companions ('B') [Stelzer et al. 2008, A&A subm.]

stars have more intense flares. A comparison of stars in Orion based on COUP and in the Cyg OB2 massive star forming region taking into account the above caveats resulted in very similar flare frequency distributions suggesting that these distributions are a universal phenomenon [15]. A further caveat to be added is that, when compared to the Sun, the observed stellar flares have very large energies, and inferring the nano-flare frequency from the above results depends on the validity of an extrapolation to small events.

THE NATURE OF CORONAE IN LIMITING REGIMES OF STELLAR DYNAMOS

The solar-type $\alpha\Omega$ -dynamo operates in the interface between radiative core and convective envelope. Therefore, solar-like magnetic activity is believed to be limited to stars with interior structure analogous to that of the Sun, and the solar-stellar analogy is expected to break down at the low- and high-mass extremes of the stellar temperature sequence. This section discusses stars at those limits, i.e. fully radiative A/B-type stars and fully convective very low-mass stars and brown dwarfs. Both groups comprise main-sequence objects and young stars on the pre-MS.

The fully radiative regime

Despite no known mechanism for the production of X-rays exists in intermediate-mass stars, ever since the early days of the *Einstein* Observatory a good fraction of them has been detected in X-rays. As the early X-ray missions had poor spatial resolution, it was argued that these stars might have late-type companions that are responsible for the X-ray emission but are not resolved from the A/B-type primaries [16].

A recent archival study of *ROSAT* data of all A-type stars from the Bright Star Catalog, constituting the sample with the highest statistics every studied for this purpose, has shown that the X-ray detection fraction is $\sim 10 - 15\%$ throughout all A/B spectral types

[17]. No differences are found in the X-ray statistics of (magnetic) Ap stars with respect to normal A-type stars, favoring the companion hypothesis.

[18, 19] have examined the possibility of a magnetic origin of the X-ray emission from A-type stars by comparing X-ray and magnetic field measurements. Most of the results support the companion hypothesis: (i) no difference between known doubles and presumed single stars in terms of X-ray luminosity vs. field strength, (ii) no difference in magnetic field strength for X-ray bright stars and upper limit sources, (iii) several arcseconds offset between the *ROSAT* X-ray source and the optical position of the A-type stars. On the other hand, in a high spatial resolution imaging study with *Chandra* many A- and B-type stars are X-ray sources although resolved from all known late-type companions [20].

Similar studies were lately carried out for intermediate-mass stars on the pre-MS (Herbig stars) with a surprising 100 % detection rate for the primary in a sample of 9 Herbig binaries or multiples [Stelzer et al. 2008, A&A subm.]; see Fig. 2. Contrary to the case of the main-sequence (MS) B/A-type stars, there is a variety of possible scenarios for X-ray production of Herbig stars: Next to the possibility of companions, these stars have relatively strong winds, some are accreting, and last but not least, magnetic fields have been detected on about 5 – 10 % of Herbig stars. The nature and geometry of these fields is not yet known. Detailed X-ray diagnostics from high-resolution spectroscopy, available so far for only one Herbig star [21], is needed to examine the source density, temperature and variability, parameters that are crucial to distinguish between different emission mechanisms.

The fully convective regime

According to standard evolutionary models, MS stars with spectral type later than $\sim M3$ are fully convective, and if any magnetic activity is to be maintained, the $\alpha\Omega$ -dynamo must be replaced by alternative mechanisms for field generation. For *young* very-low mass stars and brown dwarfs contributions to the X-ray emission from accretion may be suspected. Among the four brown dwarfs in the TW Hya association the only known accretor 2M 1207 has a very faint upper limit to its X-ray luminosity, while the non-accretor TWA 5B is a relatively bright X-ray source (see Table 1). Albeit not statistically sound, these observations are in line with results for higher mass T Tauri stars (TTS), where weak-line TTS are on average X-ray brighter than classical TTS [e.g. 22].

Larger samples of young brown dwarfs in the same star forming environment were observed e.g. during COUP and XEST, allowing to compare their fractional X-ray luminosities L_x/L_{bol} to those of higher-mass TTS. When the least-square fits of L_x/L_{bol} vs. mass obtained for the objects above the substellar limit is extrapolated into the brown dwarf regime it is in reasonable agreement with the data (Fig. 3), suggesting that there is no dramatic change in the activity level of brown dwarfs with respect to low-mass stars at ages of few Myrs. This can possibly be explained by the fact that both types of objects are fully convective, such that presumably the same kind of dynamo is at work. Better constraints on the large fraction of upper limits among the brown dwarfs are needed to

TABLE 1. 10% width of H α emission as accretion proxy and X-ray luminosity as activity for all known brown dwarfs in TWA.

Designation	$W_{\text{H}\alpha;10\%}$ [km/s]	L_x [erg/s]	Refs
TWA 5B	162	$4 \cdot 10^{27}$	[23, 24]
2M 1207	170...320	$< 1.2 \cdot 10^{26}$	[25, 26]
2M 1139	111	...	[23]
SSSPM 1102	194	$< 5.3 \cdot 10^{26}$	[23, 25]

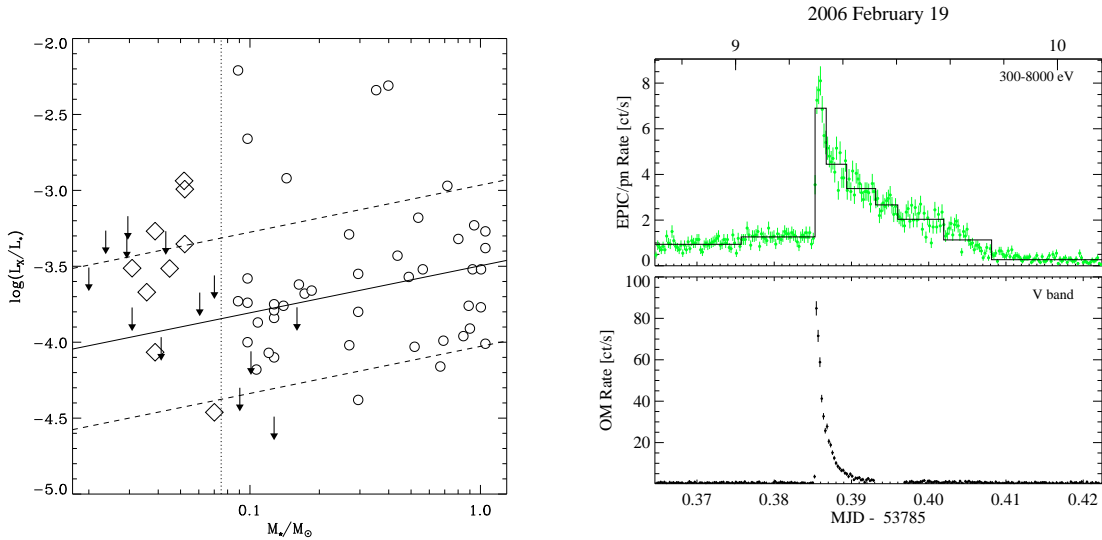


FIGURE 3. *left* - L_x/L_{bol} vs. mass for low-mass stars and brown dwarfs in the Taurus Molecular Clouds [27], *right* - giant flare on the M8 dwarf LP 412-31 observed simultaneously in X-rays and in the V band with *XMM-Newton* [28].

confirm these results.

Very few *evolved* ultracool dwarfs, i.e. stars and brown dwarfs with spectral type later than M7, have been detected in X-rays so far. Most of these detections are ascribed to flare events. A remarkable flare observation of an ultracool dwarf was obtained with *XMM-Newton* [28]. Thanks to the Optical Monitor onboard the X-ray satellite a giant flare on the M8 dwarf LP 412-31 was observed simultaneously in X-rays and in the V band (6 mag brightening); see Fig. 3. The optical peak preceded the maximum of the X-ray lightcurve by a few tens of seconds, in agreement with expectations from the standard flare scenario where chromospheric heating (giving rise to the optical flare) precedes the filling of the coronal (X-ray bright) loops. Time-resolved spectroscopy during the decay of this event allowed to study the time evolution of temperature and emission measure. Comparison to hydrodynamic flare models yields a very long loop ($\sim 1 R_\star$). Given the short flare rise time and the large loop size, the upward movement of the plasma likely involved high velocities that should give rise to line shifts observable with future X-ray missions.

HOT TOPICS ON X-RAY EMISSION FROM PRE-MAIN SEQUENCE STARS

High-resolution spectroscopic observations

XMM-Newton and *Chandra* have revolutionized our picture of stellar X-ray emission thanks to their high-resolution X-ray spectrometers that offer novel capabilities for X-ray diagnostics based on emission line analysis. Among the most compelling findings concerning cool stars was the identification of a high-density ($\sim 10^{12} \text{cm}^{-3}$) and soft excess (few MK) plasma in some classical TTS from an analysis of He-like triplets and O VII r / O VIII Ly α flux ratios, respectively:

- The *XMM-Newton*/RGS spectrum of the prototypical high-density source TW Hya [29] was successfully modeled with a composite of a normal stellar corona and a one-dimensional steady state representation of an accretion shock [30]. Anomalous low f/i ratios have confirmed high densities in nearly all classical TTS observed at high spectral resolution, the exception being T Tau (see below).
- Bright oxygen lines are useful temperature diagnostics for stellar X-ray sources. Comparison of the absorption corrected line luminosities revealed an excess of flux in the O VII resonance line for classical TTS with respect to the expected value from the O VII r / O VIII Ly α flux ratios measured for weak-line TTS and MS stars [31].

To summarize, in addition to a "normal" corona the X-ray emitting plasmas of classical TTS have a low-temperature component along with high densities, both characteristic for the physical conditions in TTS accretion shocks. In the case of T Tau there is a soft excess but no evidence for high density [32] giving rise to speculations about a suppression of coronal heating by the accretion process. Alternatively, its X-ray emission might have a different origin, such as a stellar jet. X-ray emission was, indeed, imaged with *Chandra* from the pre-MS jet of DG Tau [33]. These observations are in qualitative agreement with hydrodynamic simulations that predict a localized X-ray source from a shock at several AU from the jet launching site [34].

Effects of YSO X-rays on circumstellar matter

X-ray emission from Young Stellar Objects (YSOs) may be crucial for the structure and evolution of the circumstellar environment: (i) YSO X-rays are considered a prime ionization agent for stellar accretion disks and are held responsible for Fe K α and [Ne II] emission features that have lately been observed in a small number of objects; (ii) X-ray irradiation of close-in planets increases their mass loss rates and may lead even to complete erosion of their atmospheres.

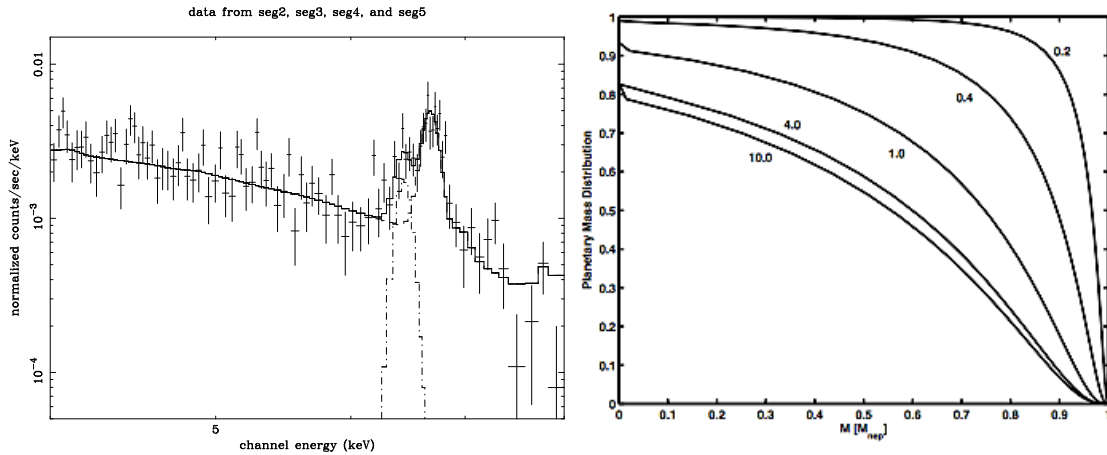


FIGURE 4. *left* - XMM-Newton EPIC spectrum with Fe K α line for the Class I protostar Elias 29 observed during DROXO [39]; *right* - Calculated mass loss of a close-in (0.02 AU) Neptune-mass exoplanet with $\rho = 2 \text{ g/cm}^3$ around a dG star at different ages of the system in Gyr [40].

Fe K α emission

Fe K α emission has been observed for several decades during solar flares. The time-profile of the 6.4 keV line from the Sun was shown to be very similar to that of soft thermal broad-band X-rays, and clearly distinct from the hard X-ray burst at the beginning of the flare [35]. This was taken as evidence that the observed Fe K α emission represents fluorescence of cold material illuminated by the corona. A natural emission site is the stellar photosphere. The same interpretation was applied to the Fe K α lines observed with *Chandra* in (no more than) two evolved stars [36, 37]. In contrast, Fe K α emission from pre-MS stars is believed to be emitted from the circumstellar disk as response to X-ray irradiation from the central star [38]. The interpretation as fluorescence emission has been questioned by [39] who found that the presence of the Fe K α line of the Class I source Elias 29 (shown in Fig. 4) is not related to the X-ray luminosity of the star.

[Ne II]12.8 μm emission

The K-shell ionization energy of Ne coincides with the peak of typical stellar X-ray spectra ($\sim 0.9 \text{ keV}$). Therefore, coronal X-rays have a high efficiency for photo-ionizing the Ne in stellar disks. Furthermore, X-ray irradiation produces a warm atmosphere above circumstellar disks with temperatures of several 1000 K, comparable to the characteristic temperatures of the infrared fine-structure transitions of low-ionized Ne [41]. The calculations by [41] predict a direct correlation between [Ne II] line flux and X-ray luminosity. First observational studies searching for this correlation in limited samples yielded controversial results [42, 43]. A systematic study based on the *Deep Rho Ophiuchus XMM-Newton Observation* (DROXO) suggests a rather complex situation with probable influence of (circum)stellar parameters such as stellar mass and accretion rate

on the Ne emission; see Flaccomio et al. in this proceedings.

Photoevaporation of planetary atmospheres

The evaporation rate of a planet atmosphere depends on the temperature in its exosphere, which may be increased by UV/X-ray irradiation from the planet host star. The irradiating high-energy flux as a function of time is therefore a crucial input to calculations of the evolution of atmospheres of close-in exoplanets. Scaling laws for the stellar X-ray luminosity as a function of age can be extracted from "The Sun in time" program [44], consisting of about a dozen solar-analogs, i.e. early G-stars from ages of 100Myr to 6.7Gyr, or from the X-ray luminosity functions of open clusters with different ages. The latter approach allows to take account of the spread in L_x of stars at a given age.

The atmospheric mass loss rate depends on the planet mass, its density, and its orbital separation (that determines the received X-ray flux). [45, 40] calculated the planet mass distribution as a function of these parameters and the (irradiation) time. An example of the results is shown in Fig. 4. Evidently, most of the mass loss takes place during the first Gyr when the X-ray luminosity is highest. To summarize, (i) the mass loss decreases with increasing size of the orbit, and becomes negligible for Neptune-mass planets beyond about 0.1 AU, (ii) at a given separation the mass loss effects are much less pronounced for planets around dM stars than for those with dG star hosts, (iii) at a given separation the evaporation is stronger for low-density planets than for high-density planets. At a separation of 0.02 AU about the majority of Neptune-like planets with low atmospheric density get eroded to Super-Earths.

All in all it seems that X-ray induced atmospheric evaporation could well be responsible for the paucity of observed close-in high-mass planets. However, a comparison of these calculations to observations has yet to be done. Such a study must be based on unbiased samples with stars of various activity levels and planets with a wide range of mass and separations.

REFERENCES

1. S. L. Baliunas, R. A. Donahue, W. H. Soon, J. H. Horne, J. Frazer, L. Woodard-Eklund, M. Bradford, L. M. Rao, O. C. Wilson, Q. Zhang, W. Bennett, J. Briggs, S. M. Carroll, D. K. Duncan, D. Figueroa, H. H. Lanning, T. Misch, J. Mueller, R. W. Noyes, D. Poppe, A. C. Porter, C. R. Robinson, J. Russell, J. C. Shelton, T. Soyumer, A. H. Vaughan, and J. H. Whitney, *ApJ* **438**, 269–287 (1995).
2. F. Favata, G. Micela, S. Orlando, J. H. M. M. Schmitt, S. Sciortino, and J. Hall, *ArXiv e-prints* **806** (2008), 0806.2279.
3. C. Isola, F. Favata, G. Micela, and H. S. Hudson, *A&A* **472**, 261–268 (2007).
4. J. Robrade, J. H. M. M. Schmitt, and F. Favata, *A&A* **442**, 315–321 (2005).
5. A. Hempelmann, J. Robrade, J. H. M. M. Schmitt, F. Favata, S. L. Baliunas, and J. C. Hall, *A&A* **460**, 261–267 (2006).
6. T. McIvor, M. Jardine, D. Mackay, and V. Holzwarth, *MNRAS* **367**, 592–598 (2006).
7. W. M. Neupert, *ApJL* **153**, L59+ (1968).
8. E. N. Parker, *ApJ* **330**, 474–479 (1988).
9. M. J. Aschwanden, T. D. Tarbell, R. W. Nightingale, C. J. Schrijver, A. Title, C. C. Kankelborg, P. Martens, and H. P. Warren, *ApJ* **535**, 1047–1065 (2000).
10. D. Berghmans, F. Clette, and D. Moses, *A&A* **336**, 1039–1055 (1998).

11. S. Krucker, and A. O. Benz, *ApJL* **501**, L213+ (1998).
12. K. V. Getman, E. Flaccomio, P. S. Broos, N. Grosso, M. Tsujimoto, L. Townsley, G. P. Garmire, J. Kastner, J. Li, F. R. Harnden, Jr., S. Wolk, S. S. Murray, C. J. Lada, A. A. Muench, M. J. McCaughrean, G. Meeus, F. Damiani, G. Micela, S. Sciortino, J. Bally, L. A. Hillenbrand, W. Herbst, T. Preibisch, and E. D. Feigelson, *ApJS* **160**, 319–352 (2005).
13. M. Güdel, K. R. Briggs, K. Arzner, M. Audard, J. Bouvier, E. D. Feigelson, E. Franciosini, A. Glauser, N. Grosso, G. Micela, J.-L. Monin, T. Montmerle, D. L. Padgett, F. Palla, I. Pillitteri, L. Rebull, L. Scelsi, B. Silva, S. L. Skinner, B. Stelzer, and A. Telleschi, *A&A* **468**, 353–377 (2007).
14. B. Stelzer, E. Flaccomio, K. Briggs, G. Micela, L. Scelsi, M. Audard, I. Pillitteri, and M. Güdel, *A&A* **468**, 463–475 (2007).
15. J. F. Albacete Colombo, M. Caramazza, E. Flaccomio, G. Micela, and S. Sciortino, *A&A* **474**, 495–504 (2007).
16. J. H. M. M. Schmitt, L. Golub, F. R. Harnden, Jr., C. W. Maxson, R. Rosner, and G. S. Vaiana, *ApJ* **290**, 307–320 (1985).
17. C. Schröder, and J. H. M. M. Schmitt, *A&A* **475**, 677–684 (2007).
18. S. Czesla, and J. H. M. M. Schmitt, *A&A* **465**, 493–499 (2007).
19. C. Schröder, S. Hubrig, and J. H. M. M. Schmitt, *A&A* **484**, 479–486 (2008).
20. B. Stelzer, N. Huéramo, G. Micela, and S. Hubrig, *A&A* **452**, 1001–1010 (2006).
21. A. Telleschi, M. Güdel, K. R. Briggs, S. L. Skinner, M. Audard, and E. Franciosini, *A&A* **468**, 541–556 (2007).
22. T. Preibisch, Y.-C. Kim, F. Favata, E. D. Feigelson, E. Flaccomio, K. Getman, G. Micela, S. Sciortino, K. Stassun, B. Stelzer, and H. Zinnecker, *ApJS* **160**, 401–422 (2005).
23. S. Mohanty, R. Jayawardhana, and D. Barrado y Navascués, *ApJL* **593**, L109–L112 (2003).
24. Y. Tsuboi, Y. Maeda, E. D. Feigelson, G. P. Garmire, G. Chartas, K. Mori, and S. H. Pravdo, *ApJL* **587**, L51–L54 (2003).
25. B. Stelzer, A. Scholz, and R. Jayawardhana, *ApJ* **671**, 842–852 (2007).
26. J. E. Gizis, and R. Bharat, *ApJL* **608**, L113–L115 (2004).
27. N. Grosso, K. R. Briggs, M. Güdel, S. Guieu, E. Franciosini, F. Palla, C. Dougados, J.-L. Monin, F. Ménard, J. Bouvier, M. Audard, and A. Telleschi, *A&A* **468**, 391–403 (2007).
28. B. Stelzer, J. H. M. M. Schmitt, G. Micela, and C. Liefke, *A&A* **460**, L35–L38 (2006).
29. B. Stelzer, and J. H. M. M. Schmitt, *A&A* **418**, 687–697 (2004).
30. H. M. Günther, J. H. M. M. Schmitt, J. Robrade, and C. Liefke, *A&A* **466**, 1111–1121 (2007).
31. M. Güdel, and A. Telleschi, *A&A* **474**, L25–L28 (2007).
32. M. Güdel, S. L. Skinner, S. Y. Mel’Nikov, M. Audard, A. Telleschi, and K. R. Briggs, *A&A* **468**, 529–540 (2007).
33. M. Güdel, S. L. Skinner, M. Audard, K. R. Briggs, and S. Cabrit, *A&A* **478**, 797–807 (2008).
34. R. Bonito, S. Orlando, G. Peres, F. Favata, and R. Rosner, *A&A* **462**, 645–656 (2007).
35. J. L. Culhane, *Irish Astronomical Journal* **15**, 69–86 (1981).
36. R. A. Osten, S. Drake, J. Tueller, J. Cummings, M. Perri, A. Moretti, and S. Covino, *ApJ* **654**, 1052–1067 (2007).
37. P. Testa, J. J. Drake, B. Ercolano, F. Reale, D. P. Huenemoerder, L. Affer, G. Micela, and D. Garcia-Alvarez, *ApJL* **675**, L97–L100 (2008).
38. M. Tsujimoto, E. D. Feigelson, N. Grosso, G. Micela, Y. Tsuboi, F. Favata, H. Shang, and J. H. Kastner, *ApJS* **160**, 503–510 (2005).
39. G. Giardino, F. Favata, I. Pillitteri, E. Flaccomio, G. Micela, and S. Sciortino, *A&A* **475**, 891–900 (2007).
40. T. Penz, G. Micela, and H. Lammer, *A&A* **477**, 309–314 (2008).
41. R. Meijerink, A. E. Glassgold, and J. R. Najita, *ApJ* **676**, 518–531 (2008).
42. I. Pascucci, D. Hollenbach, J. Najita, J. Muzerolle, U. Gorti, G. J. Herczeg, L. A. Hillenbrand, J. S. Kim, J. M. Carpenter, M. R. Meyer, E. E. Mamajek, and J. Bouwman, *ApJ* **663**, 383–393 (2007).
43. F. Lahuis, E. F. van Dishoeck, G. A. Blake, N. J. Evans, II, J. E. Kessler-Silacci, and K. M. Pontoppidan, *ApJ* **665**, 492–511 (2007).
44. I. Ribas, E. F. Guinan, M. Güdel, and M. Audard, *ApJ* **622**, 680–694 (2005).
45. T. Penz, and G. Micela, *A&A* **479**, 579–584 (2008).